

RSC Advances



This is an *Accepted Manuscript*, which has been through the Royal Society of Chemistry peer review process and has been accepted for publication.

Accepted Manuscripts are published online shortly after acceptance, before technical editing, formatting and proof reading. Using this free service, authors can make their results available to the community, in citable form, before we publish the edited article. This *Accepted Manuscript* will be replaced by the edited, formatted and paginated article as soon as this is available.

You can find more information about *Accepted Manuscripts* in the [Information for Authors](#).

Please note that technical editing may introduce minor changes to the text and/or graphics, which may alter content. The journal's standard [Terms & Conditions](#) and the [Ethical guidelines](#) still apply. In no event shall the Royal Society of Chemistry be held responsible for any errors or omissions in this *Accepted Manuscript* or any consequences arising from the use of any information it contains.



Journal Name

ARTICLE

Nickel Nanocomposites. Magnetic and Catalytic Properties

C. Castillo,^a K. Seguin,^b P. Aguirre,^a D. Venegas-Yazigi,^{c,d} A. D. C. Viegas,^e E. Spodine,^{*a,c}
V. Paredes-García^{*b,c}

Received 00th January 20xx,
Accepted 00th January 20xx

DOI: 10.1039/x0xx00000x

www.rsc.org/

In this work we are reporting the synthesis and characterization of nanocomposites obtained from the direct reduction of nickel(II) salts on matrices of polyethylene (Pe) and chitosan (Ch) in the presence of serine, under solvothermal conditions. Using different molar ratios between the metal salt (M) and amino acid (AA), eight nanocomposites were prepared, **Ni-Pe1**; **Ni-Pe2**; **Ni-Pe3**; **Ni-Pe4** and **Ni-Ch1**; **Ni-Ch2**; **Ni-Ch3**; **Ni-Ch4** (M:AA= 1:1, (1); 0.5:1, (2); 0.25:1, (3) and 0.125:1, (4)). The synthesized composites were characterized by X-ray powder diffraction techniques identifying in all cases the peaks associated to the matrix (Pe or Ch) and three peaks at 2θ values of 44.5, 51.9, 76.4°, which correspond to the Miller indices (111), (200), (220), characteristic of a face centred cubic Ni⁰ phase. The SEM images of the composites show that the use of an organic matrix changes the size and distribution of the metallic particles, being possible to observe in all cases a homogenous dispersion of the Ni⁰-NPs on the matrix surfaces. While the spherical shape observed for isolated Ni⁰-NPs is retained on the matrices, the size of the metallic particles is smaller than 100 nm, and with a less size variability, as compared with the isolated Ni⁰-NPs. All composites have a weak ferromagnetic behaviour with similar hysteresis loops, presenting H_c values ranging from 120 to 226 Oe, and reaching saturation at approximately 3 kOe. Preliminary catalytic properties for the hydrogen transfer reaction were also investigated, showing that the composites have an important activity in the transformation of acetophenone to 1-phenylethanol.

Introduction

Magnetic nanoparticles are widely studied because they exhibit interesting electrical, magnetic and chemical properties, which differ from those observed for bulk materials. Different synthetic techniques controlling the size, shape and morphology of nanoparticles have been reported [1-10], being the most used, the chemical vapour deposition (CVD) [2], wet chemistry [3], laser-driven aerosol [4], and hydro/solvothermal methods [5-6], and the micro emulsion synthetic route [7-8]. Metallic nanoparticles are mainly used in the preparation of catalysts, batteries and magnetic materials for data storage [1]. Specifically, nickel is an important magnetic material, exhibiting variable magnetism at room temperature, being the magnetic properties strongly affected by the morphology, size and shape of nickel nanoparticles [11-15]. In addition, nickel nanoparticles have interesting applications in the

growth of carbon nanotubes [16] and in the catalysis of the reduction reaction of different organic functional groups [17]. However, the catalytic properties of nickel nanoparticles have been studied less frequently compared to those of noble metals [18]. Literature data report that the nickel nanoparticles have been used as catalysts in the hydrogen transfer reaction to carbonyl groups, and hydrogenation of nitrobenzene, being both reactions of great industrial importance [19, 20]. The preparation of alcohols from carbonyl compounds has numerous applications in the industrial synthesis of dyes, pharmaceuticals, agrochemicals and biologically active compounds [21]. Therefore, the development of new and efficient catalysts for this type of reactions is a great challenge. However, the use of nickel nanoparticles as catalysts requires avoiding their oxidation. Therefore, the metallic nanoparticles have to be supported on different matrices to reach the necessary stability. Nickel nanoparticles supported on different matrices, such as carboxymethyl cellulose [22], hydrocalcite-clay [23], TiO₂, Al₂O₃, SiO₂, zeolites/aluminosilicates, chitosan and carbon nanotubes have been reported [24-29], thus generating new and interesting nickel-based materials. These systems have been studied in relation to their role not only in heterogeneous catalysis, but also for the dependence of their catalytic activity with size, shape and dispersion in the used matrix [30].

On the other hand, polymeric nanocomposites obtained from nanoparticles and polymeric matrix, are interesting due to the chemical nature and the structure of polymers should change the shape and size of the nanoparticles. In addition, the intrinsic

^a Facultad de Ciencias Químicas y Farmacéuticas, Universidad de Chile, Santiago, Chile.

^b Universidad Andres Bello, Departamento de Ciencias Químicas, Santiago, Chile.

^c CEDENNA, Santiago, Chile.

^d Facultad de Química y Biología, Universidad de Santiago de Chile, Santiago, Chile.

^e Instituto de Física, Universidade Federal do Rio Grande do Sul, Porto Alegre, Brasil.

Electronic Supplementary Information (ESI) available: Figure 1S. X-Ray powder diffraction pattern of nickel nanocomposites. Figure 2S. EDX spectra of (a) Ni-Pe1 ; (b) Ni-Ch1. Figure 3S. SEM images of nickel nanocomposites (a) Ni-P2 ; (b) Ni-P4 ; (c) Ni-C2 ; (d) Ni-C4]. See DOI: 10.1039/x0xx00000x

characteristic of the matrix should also have influence on the distribution of the nanoparticles in a polymeric matrix. Therefore, considering the relevance and applications of the nickel nanoparticles, in this work we report the synthesis of nanocomposites obtained from the direct reduction of nickel(II) chloride on matrices of polyethylene (**Pe**) and chitosan (**Ch**). Both matrices were chosen considering the chemical differences between them. To evaluate the role of the organic matrices on the obtained products, the synthesized **Ni-Pe** and **Ni-Ch** composites were morphologically and magnetically characterized. Additionally, the catalytic activity for the hydrogen transfer reaction was also investigated, showing that the composites have an important activity in the transformation of acetophenone to 1-phenylethanol.

Experimental

All starting materials were commercially available reagents of analytical grade, and were used without further purification. The Ni⁰ nanoparticles were obtained using the same synthetic conditions as reported by Paredes-Garcia et al. [6]. The composites were obtained, incorporating a constant amount (0.15 g) of the polyethylene (**Pe**) or chitosan (**Ch**) matrix to a solution of nickel(II) chloride in dimethylformamide, in the presence of L-serine, and heating the mixture at 150 °C under solvothermal conditions. Different molar ratios of metal salt (NiCl₂·6H₂O) and amino acid (AA= L-serine) were used, and the following composites were obtained: **Ni-Pe1**; **Ni-Pe2**; **Ni-Pe3**, **Ni-Pe4** and **Ni-Ch1**; **Ni-Ch2**; **Ni-Ch3**; **Ni-Ch4** (M: AA = (1), 1: 1; (2), 0.5: 1; (3), 0.25: 1 and (4), 0.125: 1). The polyethylene and chitosan composites were characterized by powder X-ray diffraction (PXRD) using a Bruker diffractometer, model D8 Advance, with Cu Kα1 radiation and Bragg-Brentano geometry in the 5° ≤ 2θ ≤ 80° range. The data were obtained at 22 °C. Carl Zeiss scanning electron microscope (SEM) with coupled energy dispersive X-ray spectroscopy (EDXS), model EVO MA10 operated at 50.0 kV and JEOL transmission electron microscope (TEM) model JEM-1001L equipment were used to characterize morphology, composition, crystal structure and size distribution of the samples.

Hydrogen transfer reaction

The catalytic hydrogen transfer reactions were performed in a magnetically stirred two necked round-bottom 50 mL flask fitted with a condenser and placed in a temperature controlled oil bath. All the reactions were carried out under nitrogen atmosphere, and repeated three times for each composite. The following reaction conditions were used for all synthesized composites: acetophenone (2 mL), isopropanol (3 mL), catalyst (30 mg) and sodium hydroxide (100 mg), which were added into the reactor, and heated at 90 °C during 3 hours. Aliquots (0.5 μL) were removed every 15 minutes, and analysed by gas chromatography. Gas chromatographic analyses were carried out with a Hewlett Packard 5890 Series II instrument, equipped with a flame ionization detector (FID) and Carbowax 20M capillary (25m×0.2mm×0.2μm), using nitrogen as carrier gas. The products were identified by spiking, using standards compounds, and by MS-GC.

Magnetic properties

Magnetic characterization was done using hysteresis cycles M(H) obtained with a vibrating sample magnetometer (VSM) and PPMS Dyna Cool 9T at room temperature, using a maximum applied field of 20 KOe. The magnetization saturation values (M_s) reported in this work was determined considering the total mass of the nanocomposites (nickel nanoparticles and matrix). The amount of nickel in each composite was calculated from the obtained M_s values, taking into consideration that the surface contribution on the M_s values is neglected, due to the large volume/surface ratio.

Results and discussion

Characterization of nanocomposites

X-Ray Powder Diffraction. The chemical nature and crystallinity of the synthesized nanocomposites was identified, using X-ray powder diffraction.

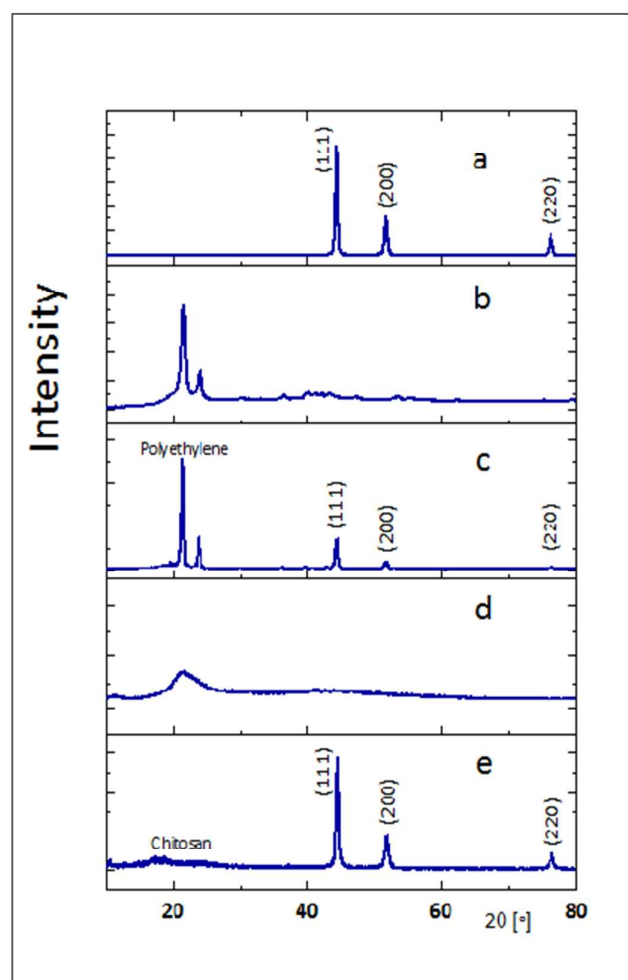


Figure 1. X-Ray powder diffraction pattern of nickel nanocomposites (a) Ni⁰-NPs; (b) Polyethylene(**Pe**) matrix; (c) Ni-**Pe1** composite; (d) Chitosan(**Ch**) matrix; (e) Ni-**Ch1** composite.

Figure 1 shows the diffraction patterns obtained for the isolated matrices (**Pe** and **Ch**) compared with two nanocomposites (**Ni-Pe1** and **Ni-Ch1**) which are representative of each used matrix. The plots are characterized by peaks associated to the matrix (**Pe** or **Ch**) and three peaks at 2θ values of 44.5 , 51.9 , 76.4° , which correspond to the Miller indices (111), (200), (220) respectively, characteristic of face centred cubic Ni^0 (JCPDS Card 04-0850, cubic system, spatial group: $Fm\bar{3}m$, $a=3.5238 \text{ \AA}$). The samples were reanalysed after one-month storage, and no changes in the number and intensity of the peaks were observed, indicating that the metallic phases are stable to ambient oxidation process. Diffraction patterns corresponding to the synthesized nanocomposites show different intensities of the peaks, which can be associated with the initial concentration of metallic salt added to the reaction mixture. The plots for the remaining phases (**Ni-Pe2**, **Ni-Pe3**, **Ni-Pe4** and **Ni-Ch2**, **Ni-Ch3**, **Ni-Ch4**) and the EDX spectra are given as supplementary material (Figure 1S and 2S).

SEM and TEM microscopy. The morphology and size of the Ni^0 -NPs were determined with the purpose to compare the structural and dispersion changes of the metallic nanoparticles as a consequence of the morphological and chemical characteristics of the organic matrix. Figure 2 shows the SEM and TEM images obtained for the Ni^0 -NPs. The micrographs permit to observe metal agglomerates with quasi spherical shape, similar to those reported by Jia et al., [31]. The size of the metallic agglomerates measured by SEM ranges from 100 to 800 nm, while in the TEM image (Figure 2b) the presence of NPs with different sizes is observed. Besides, all the particles have a thick organic coating with values between 5 to 7 nm. This coating was associated in a previous work to the amino acid used as starting materials, being also responsible of the stability of the Ni^0 -NPs, avoiding their oxidation [6].

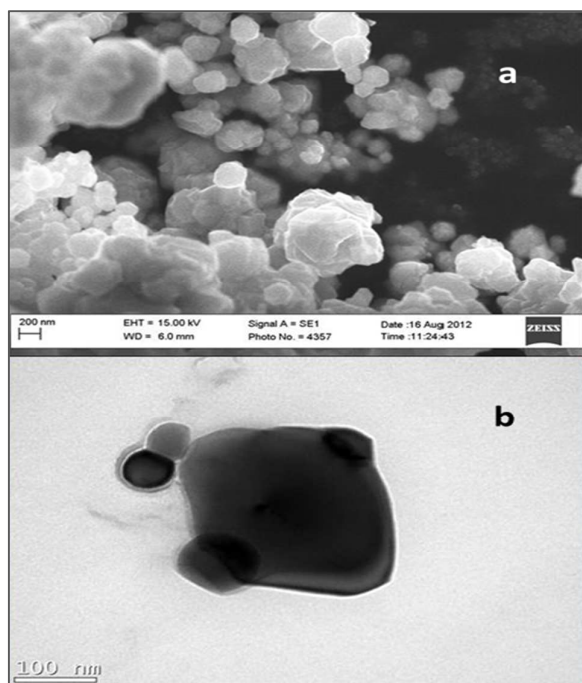


Figure 2. (a) SEM image of Ni^0 -NPs ; (b) TEM image of Ni^0 -NPs

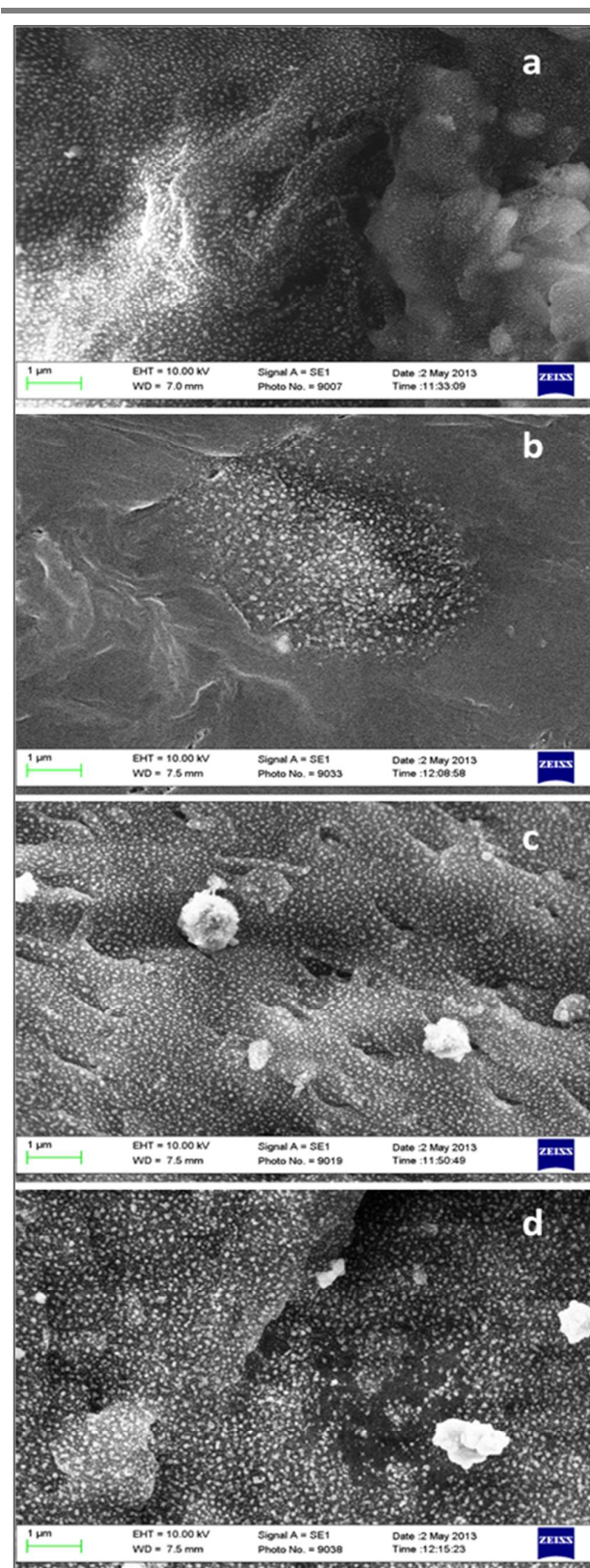
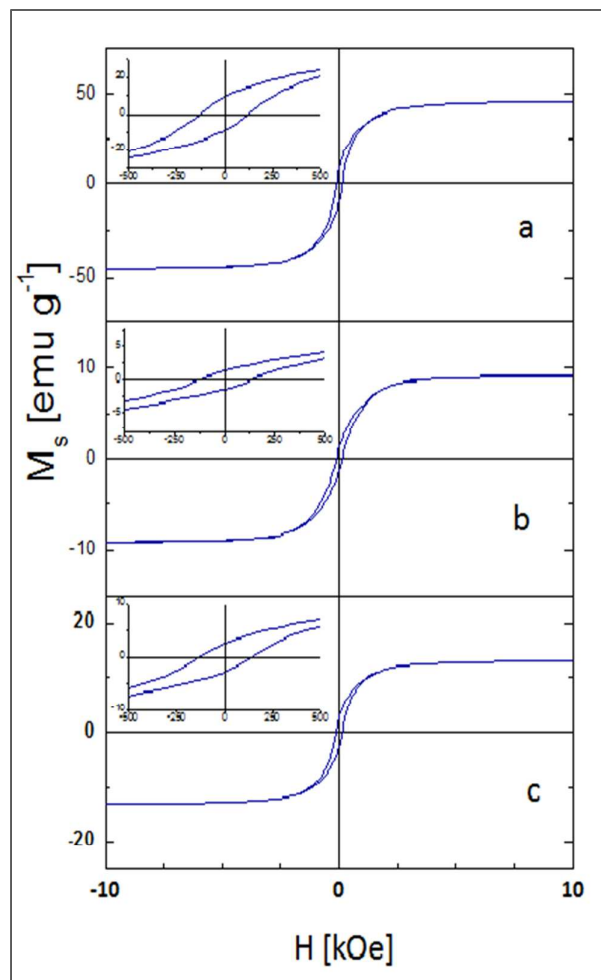


Figure 3. SEM images of nickel nanocomposites (a) **Ni-Pe1** ; (b) **Ni-Pe3** ; (c) **Ni-Ch1** ; (d) **Ni-Ch3**

Figure 3 shows the SEM images obtained for the nanocomposites **Ni-Pe1**, **Ni-Pe3**, **Ni-Ch1** and **Ni-Ch3**. The SEM images for composites **Ni-Pe2**, **Ni-Pe4**, **Ni-Ch2** and **Ni-Ch4** are given as supplementary material. The micrographs show that the use of the organic matrix changes the size and distribution of the metallic particles, showing in all cases a more homogenous dispersion as compared with the isolated Ni^0 -NPs. While the spherical shape observed for the Ni^0 -NPs is retained on the matrices, the size agglomerates is smaller than 100 nm, and with a less size variability, as compared with the Ni^0 -NPs synthesized without the presence of the organic matrices. The SEM micrographs show that in the case of nanocomposites obtained from most concentrated solutions of metallic salt, metallic nanoparticles forming agglomerates with larger sizes can be detected (Figure 3 and 3S). With a higher concentration of metallic nanoparticles (**Ni-Pe1** and **Ni-Ch1**), the dispersion in both matrices appears very similar, and considering the morphological characteristics of each matrix, no significant changes in the size or shape of Ni^0 -NPs grafted on the matrix surface are observed. However, as the concentration of the nickel nanoparticles decreases, some differences between the composites become evident. Thus, **Ni-Pe3** and **Ni-Ch3** with the same size and shape of the nanoparticles, have a completely different dispersion. Furthermore, **Ni-Ch3** retains the same dispersion distribution as **Ni-Ch1**, while **Ni-Pe3** shows important changes as compared with **Ni-Pe1**. The presence of metallic domains (islands) can be observed for this polyethylene composite, when a molar ratio M:AA of 0.25:1 is used. To the best of our knowledge this island type dispersion for nickel nanoparticles has not been reported up to date in the literature. Although, Suzuki et al., [32] and Byeon et al., [33] have used the term metallic islands or nanoscaled islands for silver and gold nanoparticles deposited on a silicon substrate, the form of the nickel island deposited in the polyethylene matrix is completely different from those reported by these authors. Comparing the samples with the lower amount of metallic nanoparticles (**Ni-Pe4** and **Ni-Ch4** (M:AA= 0.125:1), it is possible to observe some differences between the composites. No metallic islands are observed, and **Ni-Pe4** shows a more homogenous dispersion than **Ni-Ch4**. Moreover, **Ni-P4** and **Ni-Ch4** composites are characterized by not presenting large agglomerates of nickel nanoparticles. Another important aspect is the amount of the Ni^0 -NPs on the organic matrices (Table 1). According to the data, the chitosan matrix doubles the concentration of metallic nickel, as compared with the polyethylene composite. This can be related to the fact that chitosan is rich in functional groups which can interact with the nickel ions and promote the reduction process leading to the formation of the nanoparticles.

Magnetic characterization. The magnetic characterization of Ni^0 NPs, using $M(H)$ loops, was done with the purpose to compare the changes in the magnetic properties when the metallic particles are deposited on the matrices. The as synthesized Ni^0 -NPs have a soft ferromagnetic behavior with a coercivity (H_c) value of 127 Oe, saturation remanence (M_r) of 9.2 emu g^{-1} and saturation magnetization (M_s) of 46 emu g^{-1} . The values are very similar to those reported by Paredes-García et al. [6] and Jia et al., [31]. The lower value of saturation magnetization, as compared to that of

macroscopic nickel (55 emu g^{-1}) is attributed to the presence of the



organic material, which acts as coating of the nanoparticles.

Figure 4. $M(H)$ plots of (a) Ni^0 -NPs; (b) **Ni-Pe1**; (c) **Ni-Ch1**

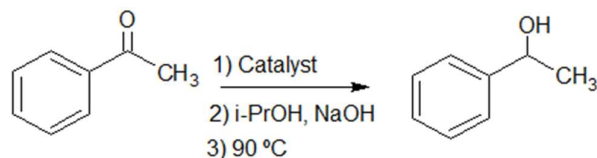
Taking into account that the M_r values depend on particle elongation, interactions effects, thermal activation, cubic magnetocrystalline and uniaxial components or formation of domain structures [34], and considering the relative large size of the particles ($> 60 \text{ nm}$) and the quasi spherical form evidenced from SEM images, it is possible to suggest that the lower remanence value observed for the synthesized nickel nanoparticles, is produced mainly by interaction effects or domain structure formation. The last is also consistent with the particle aggregation observed through the SEM images, where it is possible to observe that the distance between particles is the same as that of the diameter. Figure 4, shows the magnetic hysteresis observed for the nickel composites. All composites are characterized by having a weak ferromagnetic behaviour with H_c values such as the one obtained for Ni^0 -NPs [6], and with similar hysteresis loops reaching saturation at approximately 3 kOe. The magnetic parameters are given in table 1. In the case of polyethylene composites, **Ni-Pe1** and **Ni-Pe2** similar values of H_c ($\approx 120 \text{ Oe}$) are observed. However, **Ni-Pe3** and **Ni-Pe4** which were prepared using a lower M:AA ratio present slightly

higher coercivity values (*c.a.* 140 Oe). The same behaviour is also observed for chitosan composites being the **Ni-Ch4**, the composite with the highest H_c value (226 Oe). The higher values of the coercivity observed at lower ratio of M:AA, can be associated to the different distribution of the magnetic particles on the matrices and therefore to the interactions between them. C. Cruzat *et al.*, [35] also synthesized using chemical liquid deposition and solvated metal atom dispersive techniques, nickel nanoparticles with sizes between 10-80 nm and deposited on chitosan but, unlike this work, the authors report a superparamagnetic behaviour for the particles. Besides, Hui *et al.* [36], reported nickel nanoparticles on carbon matrix (Ni@C) with M_s values similar to those reported for **Ni-Pe1** and **Ni-Ch1** (9.2 and 13.1 emu g⁻¹ respectively). The authors explain that the lower value obtained for M_s (11.82 emu g⁻¹) for Ni@C, compared with the reported for bulk Ni⁰, is a consequence of the matrix contribution. Considering this fact, and disregarding any change of M_s on the surface, a saturation value of 55 emu g⁻¹ was taken as reference to estimate the amount of magnetic material present in the as synthesized nickel nanoparticles. The calculated value was *c.a.* 84 % being in the range obtained from TEM images if a 10 – 19 % of organic coating is considered. The same procedure was used to calculate the amount of magnetic material in the composites (Table 1).

Table 1: Magnetic parameters of nickel naocomposites

Nanocomposite	H_c [Oe]	M_s [emu g ⁻¹]	M_R/M_s	Ni [%]
Ni-Pe1	126	9.2	0.14	16.7
Ni-Pe2	122	2.1	0.13	3.8
Ni-Pe3	145	0.5	0.18	0.9
Ni-Pe4	146	0.1	0.14	0.2
Ni-Ch1	137	13.1	0.20	23.8
Ni-Ch2	140	4.8	0.18	8.7
Ni-Ch3	170	0.7	0.19	1.3
Ni-Ch4	226	0.1	0.14	0.2

Catalytic activity of nickel nanoparticles and nanocomposites. The hydrogen transfer reactions were performed using **Ni-Pe2** and **Ni-Ch2** as catalysts, which contain *c.a.* 4 and 9% of the metallic component, respectively. The catalysts were employed for heterogeneous hydrogen-transfer reactions of acetophenone, using isopropanol as hydrogen donor in the presence of NaOH (scheme 1).



Scheme 1

The catalytic study was performed taking into account the characteristics of the composites that are acting as heterogeneous

catalyst. All the experiments were performed using a same amount of composite (30 mg). Figure 5 shows the conversion as a function of the reaction time for the used catalysts. In all cases the catalytic activity starts after 15 minutes of reaction time (induction time); then the transformation of acetophenone to 1-phenylethanol gradually increases. For short reaction times, the used composites have higher conversion compared with the nickel nanoparticles, reaching at 60 minutes values of *c.a.* 55, 50 and 40 % for **Ni-Ch2**, **Ni-Pe2** and **Ni⁰-NPs**, respectively. The obtained results show that the nickel nanoparticles forming part of a composite are better catalysts in the studied reaction, compared with the coated **Ni⁰-NPs**. At 90 minutes, the conversion reaches values of 65, 48 and 55 % for **Ni-Ch2**, **Ni-Pe2** and **Ni⁰-NPs**, respectively. The selectivity for all the studied catalysts was 100%, as compared to the commercial catalyst Nickel Raney, which produces under the same experimental conditions ethylbenzene as product instead of 1-phenylethanol [37]. Furthermore, other nickel catalysts such as Ni-Al, Ni/TiO₂, Ni/SiO₂-Al₂O₃ and NiO were studied by Alonso *et al* [19] but did not present catalytic conversion towards any product. However, in this last work the reaction was run without the presence of base. The conversion value of 40% at 60 min of reaction time, observed for the as synthesized **Ni⁰-NPs** with agglomerates in the range of 100 to 800 nm, is lower than that reported by Alonso *et al.*, for spherical **Ni⁰-NPs** with a diameter of < 2 nm [19]. Thus, the importance of the size of the Ni-NPs becomes relevant, when comparing catalytic activities.

According to previous studies, when transition metals are involved, the catalytic hydrogen transfer proceeds through the hydridic route. However, Alonso *et al.* report that for **Ni⁰-NPs**, the dihydride-type mechanism is more in agreement with the data obtained with deuterated isopropanol [38]. Thus, the induction time evidenced during the first 15 min can be related with the coating of the superficial metallic particles of the composite, which must be removed, in order to permit the formation the nickel dihydride. According to the proposed mechanism, this species would be necessary for the transformation of acetophenone to 1-phenylethanol.

As can be observed in Fig. 5, the **Ni-Ch2** composite presents a higher conversion value at 60 min (65%), compared to **Ni-Pe2** and **Ni⁰-NPs**. As discussed above, the morphological characteristics of both composites **Ni-Ch2** and **Ni-Pe2** should be responsible of the difference in the catalytic activities. It is interesting to observe that at 30 min the polyethylene composite has the best catalytic activity, as compared with that of Ni-Ch2 and Ni⁰-NPs. Moreover, the same composite reaches the maximum conversion at 40 minutes, whereas the chitosan composite continues showing an increase in the conversion percentage at 90 minutes. Thus, it can be concluded that as the reaction time advances the **Ni-Ch2** composite becomes a better catalyst. It must be taken into account that the dispersion of the NPs, and molecular structure of the matrix are different in both composites, therefore the catalytic behaviour is expected to be dissimilar. Dutta *et al.*, [39] discussed the effect of the used amount of catalyst on the conversion values, and their conclusions are in accordance with those reported in this work. These authors synthesized **Ni⁰-NPs**, supported on montmorillonite, using the pores of the matrix to obtain spherical **Ni⁰-NPs** with sizes lower than 8 nm. The authors report a very high catalytic activity (using similar

reactions conditions to those of this work), obtaining a conversion near to 100% for 4 hours of reaction time. However, the conversion

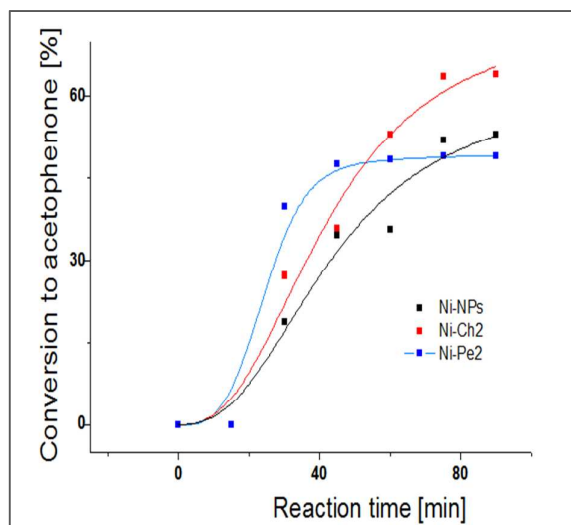


Figure 5: Conversion percentage as function of reaction time for the heterogeneous hydrogen-transfer reaction using Ni^0 -NPs, Ni-Pe2 and Ni-Ch2 as catalysts.

is only 17% after 1 hour of reaction time, being much lower than the obtained in this work (*c.a.* 50%) for both studied composites. Additionally, yolk shell type Ni^0 -NPS (Ni@SiO_2) have been studied for the same reaction at 150 °C by Park *et al.* [40]. These authors report a conversion of 90% for 1 hour of reaction. The same authors also report that the conversion value is lower when the temperature is 100 °C (68%) or 80 °C (61%); these values being in the range of those informed in this work. Moreover, Park *et al.*, also showed that the particle size affects the catalytic process, 90% of conversion at 150 °C being obtained with particles of 3 nm. This conversion decreased 10% when the particle size increased to 30 nm.

Taking into account the reported data, the catalytic activity of the synthesized composites is in agreement with the fact that the bigger size of the NPs decreases the performance of the used catalysts. However, the fact that the amount of Ni^0 -NPs on the respective studied matrices is *c.a.* half for the Ni-Pe2 composite compared to that of Ni-Ch2 , could explain the better performance of the latter at longer times of reaction if a deactivation process is considered to take place.

Conclusions

Using a solvothermal technique it was possible to synthesize Ni^0 -NPs stable to air oxidation; besides these NPs were also dispersed on chitosan and polyethylene matrices. The resulting composites present smaller size of the metallic particles, as compared with the isolated Ni^0 -NPs, making evident the role of the organic matrices on the dispersion of the magnetic particles. All composites gave a weak ferromagnetic behaviour with coercivity values ranging from 120 to 220 Oe, being classified as soft magnets. Ni^0 -NPs and the

composites Ni-Pe2 and Ni-Ch2 , were also employed as catalysts for the heterogeneous hydrogen-transfer reaction for acetophenone, reaching conversion values between 35 and 65%, depending of the reaction time. The highest conversion value was observed for Ni-Ch2 composite at 90 minutes, which may be due to the dispersion of the NPs, and molecular structure of the matrix.

Acknowledgments

The authors acknowledge CONICYT-FONDEQUIP/PPMS/EQM130086 grant and financial support from Proyecto Basal CEDENNA, Financiamiento Basal FB0807, and Laboratorio de Caracterização Magnética, LCMCM-UFSC, Departamento de Física and Centro de Microscopia Electrónica, CME-UFSC, Universidade Federal do Santa Catarina. C.C. thanks CONICYT for the Doctoral fellowship 21110032.

References

- (a) M.R. Knecht, J.C. García-Martínez, R. M. Crooks. *Chem. Mater.* 2006, **18**, 5039. (b) N. C. Nelson, T. Purnima A. Ruberu, Malinda D. Reichert. *J. Phys. Chem. C* 2013, **117**, 25826.
- C. Rui-ying. *Trans. Nonferrous Met. Soc. China.* 2006, **16**, 1223.
- Q. Zhen-Ping, G. Hong-Xia, L. Dong-Sheng, S. Xue-Ping. *J. Funct. Mater and Dev.* 2004, **10**, 95.
- H. Yuan-Qing, L. Xue-Geng, M. Swihart. *Chem. Mater.* 2005, **17**, 1017.
- L. Zhao-Ping, L. Shu, Y. You, P. Sheng, H. Zhao-Kang, Q. Yi-Tai. *Adv. Mater.* 2003, **15**, 1946.
- V. Paredes-García, C. Cruz, J. Denardín, D. Venegas-Yazigi, C. Castillo, E. Spodine, Z.Luo. *New J. Chem.* 2014, **38**, 837.
- L. Yun-Jun, L. Wei-Ping, W. Xian-Ni. *J. W. Leacher.* 2002, **2**, 20.
- G. Bao-Jiao, G. Jian-Feng, Z. Jia-Qi. *Chinese J. Inorg. Chem.* 2001, **17**, 491.
- D. Chen, S. Wu. *Chem. Mater.* 2000, **12**, 1354.
- D. Shi, P. He, P. Zhao, F. Guo, F. Wang, C. Huth, X. Chaud, S. Bud'ko, J. Lian. *Compos: Part B*, 2011, 1532.
- K. Nielsch, R. B. Wehrspohn, J. Barther, J. Kirschner, S. F. Fischer, H. Kronmüller, T. Schweinböck, D. Weiss. *U. Gosele, J. Magn. Magn. Mater.* 2002, **249**, 234.
- J. C. Bao, C. Y. Tie, Z. Xu, Q. F. Zhou, D. Shen, Q. Ma. *Adv. Mater.* 2001, **13**, 1631.
- L. Dayong, R. Shan, W. Hui, Z. Qingtang, W. Lishi. *J. Mater. Sci.* 2008, **43**, 1974.
- R. Akbarzadeh, H. Dehghani. *Dalton Trans.* 2014, **43**, 5474.
- J. Zhang, K. Yanagisawa, S. Yao, H. Wong. *J. Mater. Chem. A*, 2015, **3**, 7877.
- Yushi Qiu and Hongjuan Zheng. *J. Geng, B. Johnson, B. Zhou, S. Hermans, G. Somorjai. Nan. Sci. Tec.* 2004, **1**, 159.
- F. Alonso. *M. Yus. Chem. Soc. Rev.* 2004, **33**, 284.
- J. Geng, B. Johnson. *Nan. Sci. Tec.* 2004, **1**, 159.
- F. Alonso, P. Riente, M. Yus. *Tetrahedron.* 2008, **64**, 1847.
- F. Alonso, P. Riente, M. Yus. *Tetrahedron Lett.* 2008, **49**, 1939.
- R. Larock. "Comprehensive Organic Transformation: a Guide to Functional Group Preparations" 2nd ed. Wiley-VCH, New York.
- M. Harrad, B. Boualy, L. Firdoussi, A. Mehdi, C. Santi, S. Giovagnoli, M. Nocchetti, M. Ait. *Catal. Commun.* 2013, **32**, 92.

- 23 T. Subramanian, K. Pitchumani. *Catal. Commun.* 2012, **29**, 109.
- 24 V. Rodriguez-Gonzales, S. Alfaro, A. Zaldivar-Cadena, S.Lee. *Catal. Today.* 2011, **166**, 166.
- 25 J. Sun, X. Bao. *Chem. Eur. J.* 2008, **14**, 7478.
- 26 R. White, R. Luque, V. Budarin, J. Clark, D. Macquarrie. *Chem. Soc.* 2009, **38**, 481
- 27 J. Campelo, D. Luna, R. Luque, J. Marinas, A. Romero. *Chemsuschem.* 2009, **2**, 18.
- 28 J. De'Rogatis, M. Cargnello, V. Gombac, B. Lorenzut, T. Montini, P. Fornasiero. *Chemsuschem.* 2010, **3**, 24.
- 29 H. Sakurai, A. Murugadoss. *J. Mol. Catal. A:* 2011, **341**, 1.
- 30 M. Khairy, S. El-Safty, M. Ismael, -h. Kwarada. *Appl. Catal. B- Environ.* 2012, **127**, 1.
- 31 F. Jia, L. Zhang, X. Shang, Y. Yang. *Adv. Mater.* 2008, **20**, 1050.
- 32 Y. Suzuki, Y. Sumi, K. Kita, T. Miyanaga, K. Sagisaka. *Surf. Interface. Anal.* 2006, **38**, 1296.
- 33 J. Byeon, J. Roberts. *Langmuir.* 2014, **30**, 8770.
- 34 J. Geshev, A. Viegas, J. Echmidt. *J. Appl. Phys.* 1998, **84**, 1488.
- 35 C. Cruzat, O. Peña, M. Meléndrez, J.Díaz-Visurraga, G. Cárdenas. *Colloid. Polym. Sci.* 2011, **289**, 21.
- 36 Z. Hui, R. Zhang, X. Ying, X. Liang, T. Zhou. *Appl. Surf. Sci.* 2012, **263**, 795.
- 37 M. Andrews, C. Pillai. *Indian J. Chem. B,* 1978, **16**, 465.
- 38 (a) J.E. Bäckvall, J. Organomet. Chem. 2002, **652**, 105. (b) J. Trocha, H.B. Henbest. *Chem. Commun.* 1967, 545.
- 39 D. Dutta, B. Borah, L. Saikia, M.Pathak. *Appl. Clay. Sci.* 2011, **53**, 650.
- 40 X. J. Park, H. Lee, J. Kim, K. Park, H. Song. *J. Phys. Chem.C.* 2010, **114**, 6381.

Nickel Nanocomposites. Magnetic and Catalytic Properties

C. Castillo, K. Seguin, P. Aguirre, D. Venegas-Yazigi, A. D. C. Viegas, E. Spodine,*
V. Paredes-García*

Nickel nanocomposites are obtained under solvothermal conditions by direct reduction of nickel(II) salts on matrices of polyethylene (Pe) and chitosan (Ch) in the presence of the amino acid serine. These composites present a homogenous dispersion of the Ni⁰-NPs with sizes lower than 100 nm. The presence of metallic domains (islands) was observed when polyethylene was used as the organic matrix. All the composites can be classified as weak magnets, and are active as catalysts for the hydrogen transfer reaction for acetophenone.

